Journal of Fluorine Chemistry 185 (2016) 42–47

Contents lists available at ScienceDirect

Journal of Fluorine Chemistry

journal homepage: www.elsevier.com/locate/fluor

Short communication

First-principles molecular dynamics investigation on Na_3AlF_6 molten salt

Xiaojun Lv[a], Zhenming Xu[a], Jie Li[a,*], Jiangan Chen[b], Qingsheng Liu[c]

[a] School of Metallurgy and Environment, Central South University, Changsha 410083, China
[b] Faculty of Resource and Environmental Engineering, Jiangxi University of Science and Technology, Ganzhou 341000, China
[c] Faculty of Metallurgical and Chemical Engineering, Jiangxi University of Science and Technology, Ganzhou 341000, China

ARTICLE INFO

Article history:
Received 7 November 2015
Received in revised form 6 March 2016
Accepted 9 March 2016
Available online 15 March 2016

Keywords:
First-principles molecular dynamics
Local structure
Transport properties
Na_3AlF_6
Molten salt

ABSTRACT

Local structure and transport properties of Na_3AlF_6 molten salt were investigated by First-principles molecular dynamics (FPMD) simulation. For Na_3AlF_6 molten salt, the local ionic structure is governed by five-coordinated $[AlF_5]^{2-}$ and six-coordinated $[AlF_6]^{3-}$. Coulomb force dominates the interionic interactions for Na_3AlF_6 molten salt. The first-shell average coordination number (CN) of Na-F, Al-F in the Na_3AlF_6 molten salt is 6.03, 5.45, respectively and the F-Al-F bond angles are mainly located at 87°, 124° and 171°. The percentage of bridging F_b is small about 1–2%, while the free F_f is up to 26%, suggesting the polymerization degree of local structure is lower. Al-F bonds of the $[AlF_x]^{3-x}$ groups in Na_3AlF_6 molten salt have ionic characters as well as partial covalent characters due to the hybridization of F-2p and Al-3s (3p) orbitals, while the Na-F and F-F bonds are mainly ionic. The order of ion diffusion ability was found as $Na^+ > F^- > Al^{3+}$. Calculated results of viscosity and ionic conductivity are in good agreement with the experimental results, generally within 7%.

1. Introduction

Deep understanding about the structure and transport properties of Na_3AlF_6 molten salt has become an interesting issue, because its physical and chemical properties play key roles on the electro-deposition of Al metal from alumina in the industrial Hall–Heroult process. In addition, a better knowledge of the microscopic structure and transport properties of Na_3AlF_6 molten salt system is required for the correct interpretation of their spectroscopic data. For this reason, Na_3AlF_6 molten salt has been already investigated extensively both by theoretical simulations [1–3] and experiments [4–7]. Gilbert has reproduced the structural properties and Raman spectra of several NaF–AlF_3 crystal compounds by using interatomic potential molecular dynamics (IPMD) simulation based on the rigid ionic (RI) model, and proposed that, only the tetrahedral $[AlF_4]^-$ groups exist in $NaAlF_4$ molten salt [5]. In 2014, Serpil Cikit pointed out the five-coordinated $[AlF_5]^{2-}$ and six-coordinated $[AlF_6]^{3-}$ groups are the dominant roles in Na_3AlF_6 molten salt (cryolite) by the interatomic potential molecular dynamics (IPMD) simulation [3]. Furthermore, high temperature Raman [4,7] and NMR [5,6,8] spectrums give an alternative experimental window to insight the evolution of $[AlF_x]^{3-x}$ groups with different molten salt compositions and temperatures. The predominance of $[AlF_5]^{2-}$ in cryolite melt, proposed by Serpil Cikit is consistent with the NMR data [6]. However, the experimental measurement on molten fluoride salts can be limited by its expensive cost and strong corrosion of fluoride salt. Fortunately, computational simulation assisted with experiment provides a low cost method to explore the molten fluoride salt.

Classical IPMD has been widely applied to predict the structure and dynamic properties of Na_3AlF_6 molten salt [3,9] and other melts [10–18]. However, each new component requires fitting a set of new potential parameters, which is time consuming and limited by the inevitable indeterminacy. In addition, classical interaction potentials lose sight of the interaction between electrons, and therefore cannot be applied to study the relevant electronic property. First-principles molecular dynamics FPMD (also called as *ab initio* molecular dynamics, or AIMD) simulation has several advantages over IPMD, including the accuracy of first-principles calculation of the atomic interactions forces. FPMD therefore is flexible to study any system without needing to aforehand fit to any experimental or computed values and gets access to the full

* Corresponding author.
E-mail address: 15216105346@163.com (J. Li).

http://dx.doi.org/10.1016/j.jfluchem.2016.03.004
0022-1139/

electronic structure that is not accessible to the IPMD. Nevertheless FPMD calculation is computationally many orders of magnitude slower than IPMD, therefore it is limited to shorter simulation time and smaller system.

The combination of classical and First-principles simulation represents a very powerful tool and has been successfully applied to study these molten salts such as KCl–LiCl [19], Li_2BeF_4 [20], LiF–NaF–KF [21], $CaAl_2O_4$ [22], $CaMgSi_2O_6$ [23] and $Y_3Al_5O_{12}$ [24]. These studies to date show that FPMD simulation method can be used effectively, and Amelia Bengtson has pointed that the 216 atom unit cells and simulation time of 6–12 ps is sufficient to provide results with acceptable uncertainties and agreement with experimental data of LiCl–KCl molten salt [19]. Due to the rapid growth of computer performance, we have reasons to believe that FPMD simulation can be able to reproduce the structure and predict properties of Na_3AlF_6 molten salt.

In this paper, instead of using IPMD with the interatomic potentials, we firstly employed FPMD directly to enhance our knowledge of local structure and transport properties of Na_3AlF_6 molten salt. Firstly, details of computational method to simulate Na_3AlF_6 molten salt by FPMD are illustrated. In the results and discussions section, the basic structure-transport properties were addressed and compared with the experimental measurements to verify our FPMD model of Na_3AlF_6 melt.

2. Computational methods

2.1. Details of first-principles molecular dynamics

In this work, we employed the combination of IPMD and FPMD to improve the calculation efficiency. Initial configuration of ions system for molecular dynamics was prepared by packing ions randomly into a given simulation cell using the Packmol code [25]. We consider Na_3AlF_6 molten salt as the industrial mole component of NaF 75%, AlF_3 25%, so these simulation cells were composed of 60 Na atoms, 20 Al atoms, and 120 F atoms (a total of 200 atoms). The models of molten salt were firstly equilibrated with IPMD and then FPMD calculation initiated from the final converged structure of IPMD calculations. The method of starting FPMD calculation from the liquid prepared by IPMD has been employed successfully in the literature [26]. Note that FPMD is quite insensitive to the quality of IPMD final converged structure, so the accuracy of potential parameters used in IPMD simulation don't affect the final result of FPMD calculation. The IMPD simulations were run with the LAMMPS [27] software using the Buckingham potentials for Na_3AlF_6 molten salt system, and the potential parameters were referred from the literature [3]. Verlet Leap-Frog algorithm was used with a time step of 1 fs to solve the equation of Newton motions. Ewald sums were used for all coulomb and multipolar interactions with a buffer width of 0.5 Å and an accuracy of 10^{-5} kcal/mol [10–12]. The short-range interaction cutoff was set to 15 Å. Formal charges were used for Na (+1), Al (+3), and F (−1). The periodic boundary conditions were also applied on all sides of the model boxes to create an infinite system with no boundaries, so that the calculated results would be more convincible. To mix the system completely and eliminate the effect of initial distributions, the box systems were heated up to 4000 K in an NPT ensemble for 100 ps at 1.01 MPa, which means these simulations were run keeping the number of particles (N), pressure (P) and temperature (T) of the system constant. Then the hot liquids were cooled down at a rate of 1 K/ps to the melting point 1283 K. Another equilibrium at NPT ensemble for 100 ps was performed for relaxation. After these runs, convergence was achieved and the density difference between the initial and the final state fell below 1%.The resulting structure and velocities were used to start the following FPMD simulation.

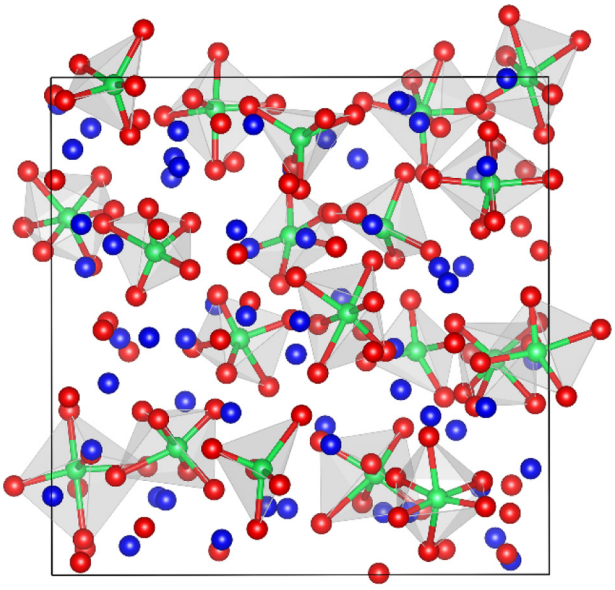

Fig. 1. Snapshot of the local ion structure in cryolite melt. F^- ions in red, Al^{3+} in green, and Na^+ in blue (For interpretation of the references to colour in this figure legend, the reader is referred to the web version of this article.).

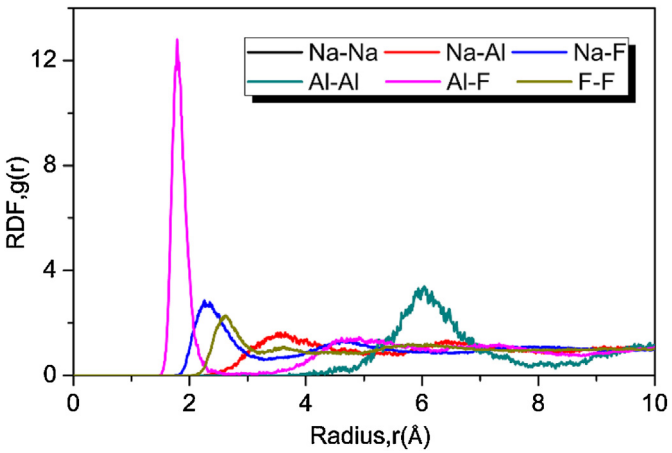

Fig. 2. Calculated Na—Na, Na—Al, Na—F, Al—Al, Al—F and F—F radial distribution functions in Na_3AlF_6 molten salt.

FPMD simulation for Na_3AlF_6 molten salt has been launched with the CASTEP (Cambridge serial total energy package) code [28,29]. Perdew–Burke–Ernzerhof (PBE) exchange-correlation function was implemented in the generalized gradient approximation (GGA) [30]. Ultrasoft pseudo potentials (USPP) have been employed for all the ion-electron interactions. The ionic cores are represented by USPP for Na, Al and F atom. The Na $2s^22p^63s^1$ electrons, Al $3s^23p^1$ electrons and F $2s^22p^5$ electrons are explicitly regarded as valence electrons. Dispersion force was also included by using the semi-empirical DFT-D2 method [19,26,31]. Energy cutoff of 350 eV and a $1 \times 1 \times 1$ *k*-point mesh was chosen for FPMD simulation. Time step for FPMD simulation was chosen at 1 fs to insure an energy drift less than 1 meV/atom/ps. FPMD simulation was done in a statistical ensemble with fixed particle number, volume and temperature (NVT) using the Nosé-thermostat [32]. The simulation temperature (1283 K, melting point of Na_3AlF_6) was similar to IPMD, and the density of simulation model was set to the experimental value [33,34] 2.095 g/cm^3. Periodic boundary condition was also employed in FPMD and simulation represent an infinite molten salt system. After FPMD being launched, the average pressure and resulting pressure in our NVT is 0.00014 and

Table 1
Comparison of the first-peak, first-minimum radius and first-shell average coordination numbers for ion pairs in Na_3AlF_6 molten salt by IPMD calculation.

Ion pair	First-peak radius		First minimum radius		Coordination number	
	FPMD	IPMD	FPMD	IPMD	FPMD	IPMD
Na—Na	3.685	3.65[a],3.55[b],3.5[d]	5.125	5.1[a],5.2[d]	8.93	9.01[d]
Na—Al	3.665	3.66[a],3.57[b],3.46[c],3.8[d]	5.125	5.0[a],5.2[d]	2.99	3.3[d]
Na—F	2.345	2.24[a],2.20[b],2.20[d]	3.275	3.4[a],3.4[d]	6.03	5.1[d]
Al—Al	6.085	3.74[a],3.59[b],5.89[c],4.1[d]	7.825	4.6[a],4.9[d]	5.3	2.0[d]
Al—F	1.785	1.78[a],1.81[b],1.75[c],2.1[d]	2.70	2.8[a],3.1[d]	5.45	6.4[b],5.62[c],6.6[d]
F—F	2.655	2.54[a],2.52[b],2.8[d]	3.205	3.1[a],3.6[d]	5.66	5.83[d]

[a] Ref. [34].
[b] Ref. [9].
[c] Ref. [3].
[d] Ref. [37].

−0.003 GPa, respectively, which means the box volume for NVT calculation is reasonable. Finally, the trajectories of all atoms were collected for the following statistical calculations of structure and transport properties.

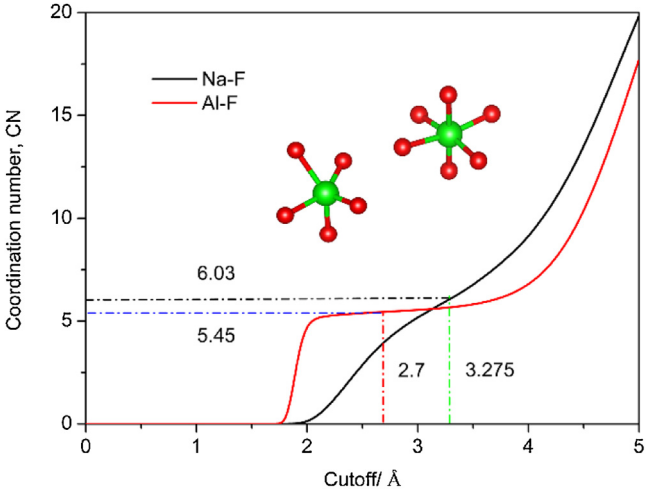

Fig. 3. First-shell coordination number function of Na—F and Al—F pairs in Na_3AlF_6 molten salt.

2.2. Statistics of structural information

The partial radial distribution function (PRDF) analysis was conducted from the MD trajectories to study the local structure surrounding a certain ion in fluoride melts. The PRDFs give the probability of finding an ion within a distance Δr from a specified particle at the location of r, and the CNs show the average coordination number (CN) for atom i around atom j [35]. The equation of PRDF is expressed as below (Eq. (3)).

$$g_{ij}(r) = \frac{V}{N_i N_j} \Sigma_j \left\langle \frac{n_{ij}(r, \Delta r)}{4\pi r^2} \right\rangle \quad (1)$$

where, V is the volume of the MD box cell and N is the number of a special particle. n_{ij} $(r, \Delta r)$ is the average number of atom j surrounding a central atom i within a defined cut-off distance Δr.

The first-shell coordination number (CN) of Al with the surrounding F anion was estimated by numerical integration of the PRDFs within a cut-off radius, which corresponds to the first minima of the corresponding partial $g_{Al\text{-}F}$ (r) [11]. We referred to the integral of PRDF as the function (Eq. (2)),

$$N_{Al-F} = 4\pi\rho_F \int_0^R r^2 g_{Al-F}(r) dr \quad (2)$$

where $g_{Al\text{-}F}$ (r) is the PRDF between species Al and F, and ρ_F the average number density of species F atom.

As for the distribution of Al(III) monomeric fluoro-complexes and fluoride atom type calculation, the Matlab program was compiled to deal with the trajectories of our FPMD simulation.

2.3. Calculation of transport properties

Through statistical analysis of the particle trajectories, function of the mean square displacement (MSD) vs time would be generated by the Einstein-Smoluchowshi equation [10].

$$\mathrm{MSD} = \left\langle \Delta \bar{r}(t)^2 \right\rangle = \frac{1}{N} \left\langle \Sigma |r_{i(t)} - r_{i(0)}| \right\rangle \quad (3)$$

where, $r_{i(t)}$ is the location of atom i at the time t, and the bracket means an ensemble average.

Combined with the statistical thermodynamics, some transport properties of molten salt such as self-diffusion coefficient D, viscosity η and ionic conductivity σ would be calculated on account of the MSD curves of particles. The relation between the self-diffusion coefficient D and the MSD curve is shown as below

Table 2
Distribution of Al(III) monomeric fluoro-complexes and fluoride atom types in cryolite melt as function of the cutoff distance (in Å), as well as with and computational [7,39] and experimental [1] results reported in the literature. For results in the two Refs. [1,39], the dimeric fluoro-complexe and fluoride-ion was considered.

Cutoff distance	$[AlF_4]^-$	$[AlF_5]^{2-}$	$[AlF_6]^{3-}$	Bridging F_b	Terminal F_t	Free F_f
2.0	0.45	0.35	0.2	0.00	0.88	0.13
2.2	0.1	0.55	0.35	0.01	0.78	0.21
2.4	0	0.60	0.40	0.01	0.76	0.23
2.6	0	0.50	0.50	0.01	0.74	0.25
2.8	0	0.45	0.55	0.02	0.73	0.26
3.0	0	0.45	0.55	0.02	0.73	0.26
Ref. [1]	0.02,0.04	0.36,0.20	0.20,0.24			
Ref. [7]	0.01	0.32	0.67			
Ref. [39]	0.04,0.02	0.16,0.34	0.52,0.36			

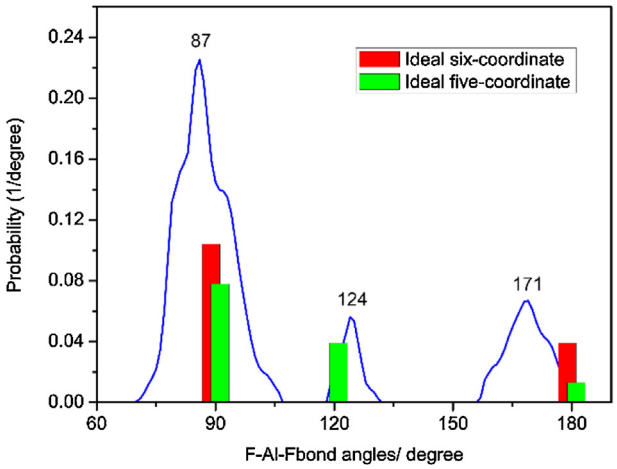

Fig. 4. The distribution probability of F—Al—F bond angles in Na_3AlF_6 molten salt.

[36].

$$D = \lim_{t\to\infty} \frac{1}{6} \frac{d\left[\Delta r(t)^2\right]}{dt} \tag{4}$$

Then the viscosity η and ionic conductivity σ can be obtained by combining the self-diffusion coefficient D with the Einstein–Stokes formula and Nernst–Einstein equation respectively [16].

$$\eta = \frac{K_B T}{2\pi D\lambda} \tag{5}$$

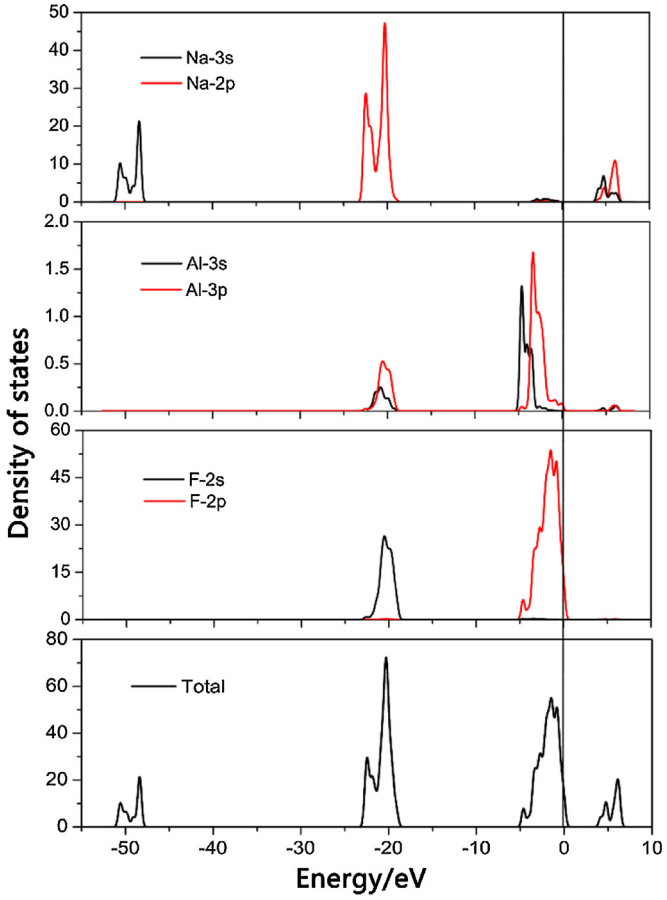

Fig. 5. Total and partial density of states (DOS) of a $[AlF_6]_4Na_{12}$ cluster. The vertical line indicates the Fermi (HOMO) energy.

$$\sigma = D\frac{nq^2}{K_B T} \tag{6}$$

where, K_B is the Boltzmann constant, which equals to 1.38×10^{-23} J/K, T is the temperature of the system, λ is the step length of ion diffusion and it is generally considered to being equal to the diameter of ion ($\lambda = 2R$), n presents the unit volume concentration of carrier atoms, which equals to the number of carrier atoms in a unit volume, and q is the charge of ion.

3. Results and discussions

3.1. Structure information

After FPMD simulation, the structural information was obtained from the statistical calculations of particles' trajectories. Fig. 1 show the snapshot of local ionic structure of Na_3AlF_6 molten salt. F^- ions are shown in red, Al^{3+} in green, and Na^+ in blue. Grey lines represent bonds between Al and F ions if their distances are less than the first minimum of the radial distribution function. In this work, "bond" is not a real chemical bond but just an atom pair within a specified distance. Fig. 1 indicates that the local ionic structure is governed by five-coordinated and six-coordinated Al species, corresponding to the distorted trigonal bipyramid and octahedral configuration. For Na_3AlF_6 molten salt, though losing long-range order, the local ion structure keeps the short-range order of five-coordinated $[AlF_5]^{2-}$ and six-coordinated $[AlF_6]^{3-}$ as same as that in Na_3AlF_6 crystal.

3.1.1. Partial radial distribution functions

The partial radial distribution functions (RDFs) of Na_3AlF_6 molten salt are shown in Fig. 2. It can be seen from Fig. 2 that the first peak of Al—F is quite sharp, indicating F^- anions around Al^{3+} are arranged in the form of ordered states. Table 1 also summarizes the calculated local structure parameters for the ion pairs in Na_3AlF_6 molten salt in comparison with other calculated values by IPMD from the literatures [3,9,34,37]. From Fig. 2 and Table 1, we observed that our calculated first-peak and first minimum radius values are in good agreement with all the previous calculated results by IPMD, while the first peak value of Al—Al is only similar to Serpil Cikit's. The first peak of Al—Al located at 6.085 Å is much

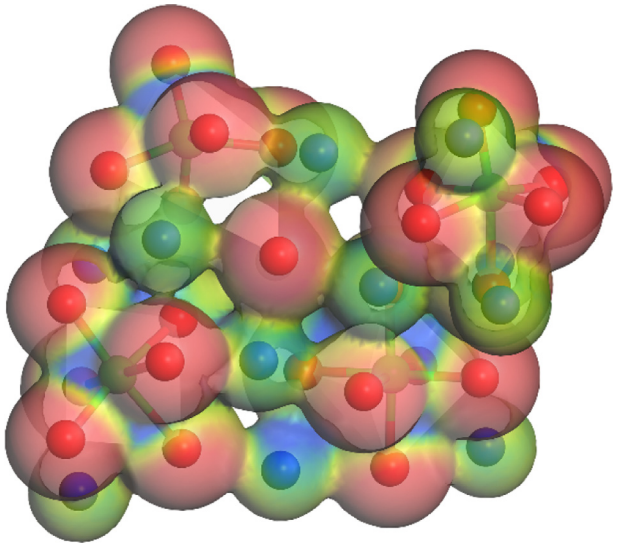

Fig. 6. Electron density of a $[AlF_6]_4Na_{12}$ cluster. Insert: The central $[AlF_6]^{3-}$ ion cluster.

Table 3
Average Mulliken atomic orbital populations (s, p), total population (total), charges transferred (charge) and overlap population of $[AlF_6]_4Na_{12}$ cluster (unit: *e*).

Atoms	s	p	Total	Charges	Bonds	Population
Na	2.12	6.04	8.16	0.84	Na—F	0.035
Al	0.46	0.76	1.21	1.79	Al—F	0.27
F	1.96	5.76	7.72	−0.72	F—F	−0.03

Table 4
Ion self-diffusion coefficients (10^{-9} m^2/s), viscosity (mPa s) and ionic conduction (S/cm) in Na_3AlF_6 molten salt.

	Self-diffusion coefficient			Viscosity	Ionic conduction
	Na	Al	F		
Present work	7.36	2.57	6.47	1.37	2.873
Reference				1.28[a]	2.8[a],2.85[b]
Factsage				1.15	

[a] Ref. [41].
[b] Ref. [40].

larger than twice that of Al-F, indicating only a few Al-Al bonds are linked by the bridging F^- anions. As for a central Al^{3+} ion, F^- anions are located at its first shell, the second shell is occupied by Na^+ ions, and the same Al^{3+} ions are in the third shell, suggesting that Coulomb forces dominate the interionic interactions for Na_3AlF_6 molten salt.

3.1.2. Coordination numbers

With the integral of ion pair's PRDF, the average CN was considered to be equal to the ordinate value (special cutoff) corresponding to the integral function. When choosing the cutoff distance of Al—F, Na—F at 2.7 Å and 3.275 Å, respectively, the average coordination numbers of Al—F (5.45), Na—F (6.03) was obtained, as shown in Fig. 3 and Table 1. The first-shell average coordination number (CN) of Al—F in Na_3AlF_6 molten salt is smaller than 6 in the Na_3AlF_6 crystal and it is well consistent with the snap shot (Figure.1) that aluminum ions are mainly in the form of five-coordinated $[AlF_5]^{2-}$ and six-coordinated $[AlF_6]^{3-}$.

The distributions of Al(III) monomeric fluoro-complexes were obtained by calculating the percentage of an Al^{3+} ion having a given number of neighbors (F^- anions) from all the trajectories of FMMD simulation. Neighbors are these ions which are located inside the first shell corresponding to the position of the minimum of the PRDF illustrated in Fig. 2. Table 2 shows the percentage of Al^{3+} ions in the four-coordinated, five-coordinated, or six-coordinated structure and the F atom type in Na_3AlF_6 molten salt. It is observed that the six-coordinated $[AlF_6]^{3-}$ groups are the dominant species about 55% in Na_3AlF_6 molten salt with the cutoff of 2.8 Å, corresponding to the distorted octahedral configuration. This result agrees with those deduced from the experimental Raman spectrum, asserting that the six-coordinated aluminum complexes $[AlF_6]^{3-}$ are the major species in molten cryolite [38]. While cutoff $\leq$ 2.6 Å, five-coordinated $[AlF_5]^{2-}$ ions are the protagonists up to 50–60% in Na_3AlF_6 molten salt, and the percentage of $[AlF_6]^{3-}$ lies in 35–50%. Besides, when cutoff $\geq$2.4, the percentage of $[AlF_4]^-$ is zero, what is certain is that four-coordinated $[AlF_4]^-$ is quite rare in Na_3AlF_6 molten salt. Although a difference of dimeric fluoro-complex and fluoride-ion being considered, the data reported in the experimental and computational [1,7,39] works agree with our calculated results and support above conclusions.

The F atom type (bridging F_b, terminal F_t and free F_f) measures the structure polymerization degree of Na_3AlF_6 molten salt and has a significant impact on the transport properties. In Table 2, it can be seen that, the percentage of bridging F_b is smaller about 1–2% and the free F_f is up to 26%, suggesting the polymerization degree of ionic structure is lower. This is consistent with the fact the first peak of Al—Al pair's PRDF located at 6.08 Å is much larger than twice that of the Al—F.

3.1.3. Bond angles distributions

Following Fig. 4 shows the angle distributions of F-Al-F bonds in Na_3AlF_6 molten salt at 1283 K extracted from the simulation data, compared with the ideal trigonal bipyramidal $[AlF_5]^{2-}$ and octahedron $[AlF_6]^{3-}$. Here, the ideal trigonal bipyramidal $[AlF_5]^{2-}$ have the F—Al—F angles of 90° × 6, 120° × 3, and 180° × 1, and the ideal octahedron $[AlF_6]^{3-}$ have the F—Al—F angles of 90° × 8 and 180° × 3. The main peak and second peak of F—Al—F distribution located at 87° and 171°, respectively correspond to an octahedron or trigonal bipyramidal configuration. Moreover, the third peak around 124deg exclusively points to the trigonal bipyramidal configuration. However, all these peaks are slightly deviated from that characters in ideal configuration, indicating these trigonal bipyramidal and octahedron configurations are partly distorted. As expected, no peak of 109° demonstrates the existence of tetrahedron $[AlF_4]^-$.These calculated angle distributions confirm that Al—F bonds principally exist in the distorted trigonal bipyramidal and octahedron in Na_3AlF_6 molten salt.

3.2. Electronic structure of the $[AlF_6]^{3-}$ cluster

In Na_3AlF_6 molten salt system, $[AlF_6]^{3-}$ cluster is the dominant species according to our FPMD simulation. To insight the electronic structure properties such as density of state, electron density and Mulliken population, quantum chemical calculations for the selected $[AlF_6]_4Na_{12}$ cluster from a certain MD trajectory were carried out. In a typical cluster of $[AlF_6]_4Na_{12}$, the central $[AlF_6]^{3-}$ complex is surrounded by a second solvation shell with a total of three Na^+ ions. Total and partial density of states (DOS) of a $[AlF_6]_4Na_{12}$ cluster were obtained, as shown in Fig. 5. The orbitals near core with lowest energy around−50 eV were occupied by Na-3s states and orbitals with middle energy around−20 eV were occupied by Na-2p and F-2s states. In addition, the orbitals near the Fermi (HOMO) level is essentially dominated by F-2p states, with an admixture with Al-3s, 3p states. It indicates that some covalent bonding interactions (Al—F) exist in the $[AlF_6]^{3-}$ cluster and the possibility of electrons to transit from Al-3s, 3p to F-2p states. Fig. 6 shows the electron density of a $[AlF_6]_4Na_{12}$ cluster, the electrons transferring from the central Al atoms and surrounding Na atoms are mainly localized at F atoms, implying the distinct Coulomb interactions exist in the $[AlF_6]_4Na_{12}$ cluster. Averaged Mulliken populations of the $[AlF_6]_4Na_{12}$ cluster are displayed in Table 3. The bond population of Al—F is 0.27, which is greater than that value of 0.035 of Na-F bond, implying the covalent character of the former is more evident than the latter. It is characteristic for Al—F bonds having ionic characters as well as partial covalent characters due to the hybridization of F-2p and Al-3s (3p) orbitals, while Na—F and F—F bonds are mainly ionic. These are in agreement with the results of above density of states (DOS) analysis.

3.3. Transport properties

With the computational methods in section 2.3, MSD cures of Na_3AlF_6 molten salt were obtained. One sixth of the slope of MSD cure in the linear region represents the ion self-diffusion coefficient, and corresponding results were shown in Table 4. The viscosity of electrolyte affects the separating effect between liquid metal, solid slag, gas and electrolyte. In the production of aluminum electrolysis, it's preferable to keep an appropriately lower viscosity of the electrolyte for better separation between aluminum liquid and electrolyte. The viscosity η, which measures

the resistance of a fluid to being deformed by shear stress, can be calculated by combining the self-diffusion coefficients D of all Na^+, Al^{3+}, F^- ions and Einstein–Stokes approximation, and the step length λ of ion diffusion is considered to be equal to the diameter of Na^+, Al^{3+}, F^- ion (so λ = 2.04, 1.07 and 2.66 Å). Na_3AlF_6 molten salt have a relatively high self-diffusion coefficient, so it has outstanding liquidity and ionic conductivity. Increasing the ionic conductivity of aluminum electrolyte can improve the current efficiency and then reduce energy consumption. As one of the most important properties of electrolyte, ionic conductivity σ was calculated by self-diffusion coefficients D and the Nernst–Einstein approximation. Our calculated results of viscosity η and ionic conductivity σ compared to the experimental values at 1300 K from the literatures [40,41] and our Factsage thermodynamic calculated result are all listed in Table 4.

It can be observed from Table 4 that the order of ion diffusion ability is found as $Na^+ > F^- > Al^{3+}$. The self-diffusion coefficients of Na^+ ion is three times as large as Al^{3+} ion. The movement ability of ions is not only affected by the ionic radius, but depends on the surrounding atomic interactions. Na^+ ions have smaller radius and are free only for electrostatic interactions with surrounding particles, while $Al^{3+}$and F^- ions exist in the form of $[AlF_x]^{3-x}$, having larger volume and resistance to motion. Table 4 shows the calculated results of viscosity η = 1.37 mPa s are in good agreement with the experimental results of 1.28 mPa s by Janz [41] and our Factsage thermodynamic calculation of 1.15 mPa s. In addition, the calculated result of ionic conductivity σ = 2.873 S/cm of Na_3AlF_6 molten salt is also in fairly good agreement with the experimental value of 2.8 S/cm and theoretical calculation data of 2.85 S/cm, generally within 2.6%.

As we know, the MD simulation of transport property is fastidious about the ionic structure, so the accuracy of transport property can represent the success of MD simulation. In view of our calculated results of total radial distribution function, viscosity and ionic conductivity are in fairly good agreement with experimental values, generally within 7%, the conclusion can be made that our FPMD simulation for structure and transport properties of Na_3AlF_6 molten salt are reasonable.

4. Conclusion

First-principles molecular dynamics FPMD simulation were carried out to expand our knowledge of key structure and transport properties of Na_3AlF_6 molten salt. The partial radial distribution function, coordination numbers, bond angles, F atoms type, self-diffusion coefficient, viscosity and ionic conduction were studied and compared to the experimental results to verify the FPMD simulation of Na_3AlF_6 molten salt.

For Na_3AlF_6 molten salt, though losing long-range order, the local ion structure keeps the short-range order of five-coordinated $[AlF_5]^{2-}$ and six-coordinated $[AlF_6]^{3-}$. However, the four-coordinated $[AlF_4]^-$ is quite rare in Na_3AlF_6 molten salt. The first peak of Al—Al located at 6.085 Å is much larger than twice that of the Al-F, indicating only few Al—Al bonds are linked by bridging F^- anion. Coulomb forces dominate the interionic interactions for Na_3AlF_6 molten salt. The first-shell average coordination number (CN) of Al-F in Na_3AlF_6 molten salt is 5.45 and the F—Al—F bond angles are mainly located at 87°, 124° and 171°. The percentage of bridging F_b is small about 1–2% and the free F_f is up to 26%, suggesting the polymerization of ionic structure is lower.

According to quantum chemical calculations, Al—F bonds of the $[AlF_x]^{3-x}$ groups in Na_3AlF_6 molten salt have ionic interactions as well as partial covalent characters due to the hybridization of F-2p and Al-3s (3p) orbitals, while Na—F and F—F bonds are mainly ionic characters. The order of ion diffusion ability was found as $Na^+ > F^- > Al^{3+}$ and the self-diffusion coefficients of Na^+ ions is three times as large as Al ions. Our calculated results of viscosity and ionic conductivity are in fairly good agreement with the experimental results, generally within 7%. In sum, our FPMD simulation for structure and transport properties Na_3AlF_6 molten salt are reliable.

Acknowledgements

We sincerely acknowledge the High Performance Computing Center of CSU, China. This work was financially supported by the National Science and Technology Support Project of China (No. 2012BAE08B02) and National Natural Science Foundation of China (No. 51264011).

References

[1] R.R. Nazmutdinov, T.T. Zinkicheva, S.Y. Vassiliev, D.V. Glukhov, G.A. Tsirlina, M. Probst, Spectrochim. Acta A 75 (2010) 1244–1252.
[2] R.R. Nazmutdinov, T.T. Zinkicheva, S.Y. Vassiliev, D.V. Glukhov, G.A. Tsirlina, M. Probst, Chem. Phys. 412 (2013) 22–29.
[3] S. Cikit, Z. Akdeniz, P.A. Madden, J. Phys. Chem. B 118 (2014) 1064–1070.
[4] B.M. Gilbert, Appl. Spectrosc. 44 (1990) 299–305.
[5] B. Gilbert, E. Robert, E. Tixhon, J.E. Olsen, T. Østvold, Inorg. Chem. 35 (1996) 4198–4210.
[6] E. Robert, V. Lacassagne, C. Bessada, D. Massiot, B. Gilbert, J.-P. Coutures, Inorg. Chem. 38 (1999) 214–217.
[7] Z. Akdeniz, Paul A. Madden, J. Phys. Chem. B 110 (2006) 6683–6691.
[8] V. Lacassagne, C. Bessada, P. Florian, S. Bouvet, B. Ollivier, J.-P. Coutures, D. Massiot, J. Phys. Chem. B 106 (2002) 1862–1868.
[9] D.K. Belashchenko, O.I. Ostrovski, S.Y.U. Saposznikova, Metall. Mater. Trans. B 29B (1998) 105–110.
[10] N. de Koker, Geochim. Cosmochim. Acta 74 (2010) 5657–5671.
[11] F.J. Spera, M.S. Ghiorso, D. Nevins, Geochim. Cosmochim. Acta 75 (2011) 1272–1296.
[12] F.J. Spera, D. Nevins, M. Ghiorso, I. Cutler, Geochim. Cosmochim. Acta 73 (2009) 6918–6936.
[13] G. Malavasi, A. Pedone, M.C. Menziani, J. Phys. Chem. B 117 (2013) 4142–4150.
[14] T.R. Stechert, M.J.D. Rushton, R.W. Grimes, A.C. Dillon, J. Non-Cryst. Solids 358 (2012) 1917–1923.
[15] H. Rezvantalab, G. Drazer, S. Shojaei-Zadeh, J. Chem. Phys. 142 (2015) 014701.
[16] T. Wu, S. He, Y. Liang, Q. Wang, J. Non-Cryst. Solids 411 (2015) 145–151.
[17] P. Zhang, W. Hui, Y. Zhang, X. Ren, D. Zhang, J. Non-Cryst. Solids 358 (2012) 1465–1473.
[18] G. Lusvardi, G. Malavasi, M. Cortada, L. Menabue, M.C. Menziani, A. Pedone, U. Segre, J. Phys. Chem. B 112 (2008) 12730–12739.
[19] A. Bengtson, H.O. Nam, S. Saha, R. Sakidja, D. Morgan, Comput. Mater. Sci. 83 (2014) 362–370.
[20] A. Klix, A. Suzuki, T. Terai, Fusion Eng. Des. 81 (2006) 713–717.
[21] H.O. Nam, A. Bengtson, K. Vörtler, S. Saha, R. Sakidja, D. Morgan, J. Nucl. Mater. 449 (2014) 148–157.
[22] V. Cristiglio, L. Hennet, G.J. Cuello, I. Pozdnyakova, M.R. Johnson, H.E. Fischer, D. Zanghi, D.L. Price, J. Non-Cryst. Solids 354 (2008) 5337–5339.
[23] N. Sun, L. Stixrude, N.d. Koker, B.B. Karki, Geochim. Cosmochim. Acta 75 (2011) 3792–3802.
[24] V. Cristiglio, L. Hennet, G.J. Cuello, M.R. Johnson, A. Fernández-Martínez, H.E. Fischer, I. Pozdnyakova, D. Zanghi, S. Brassamin, J.F. Brun, D.L. Price, J. Non-Cryst. Solids 353 (2007) 1789–1792.
[25] L. Martinez, R. Andrade, E.G. Birgin, J.M. Martinez, J. Comput. Chem. 30 (2009) 2157–2164.
[26] G. Kresse, J. Hafner, Phys. Rev. B 47 (1993) 558–561.
[27] S. Plimpton, J. Comput. Phys. 117 (1995) 1–19.
[28] D.J.G. Kresse, Phys. Rev. B 59 (1999) 1758–1775.
[29] G. Kresse, Phys. Rev. B 54 (1996) 169–186.
[30] K.B. John, P. Perdew, Matthias Ernzerhof, Phys. Rev. Lett. 77 (1996) 3865–3868.
[31] J. Klimeš, D.R. Bowler, A. Michaelides, Phys. Rev. B 83 (2011).
[32] S. Nosé, J. Chem. Phys. 81 (1984) 511.
[33] G.J. Janz, R.P.T. Tomkins, J. Phys. Chem. Ref. Data 12 (1983) 591.
[34] W.B. Frank, L.M. Foster, J. Phys. Chem. 64 (1960) 95–98.
[35] J.M. Ziman, Principles of the Theory of Solids Cambridge, Cambridge University Press, Cambridge University, 1972.
[36] R. Kubo, Rep. Prog. Phys 29 (1966) 255–284.
[37] H. Hou, G.X.S. Chen, X. Zhang, Chin. J. Nonferrous Met. 10 (2000) 914–917.
[38] Z.M. Akdeniz, P.A. Madden, J. Phys. Chem. B 110 (2006) 6683–6691.
[39] Frédéric Bouyer, Gérard Picard, Int. J. Quantum Chem. 61 (1997) 507–514.
[40] P. Fellner, O. Kobbeltvedt, Å. Sterten, J. Thonstad, Electrochim. Acta 38 (1993) 589–592.
[41] G.J. Janz, R.P.T. Tomkins, J. Phys. Chem. Ref. Data 5 (1983) 591–815.